Characterization of the Sources of Protein-Ligand Affinity: 1-Sulfonato-8-(1′)anilinonaphthalene Binding to Intestinal Fatty Acid Binding Protein

William R. Kirk, Elizabeth Kurian, and Franklyn G. Prendergast
Department of Pharmacology, Mayo Foundation, Rochester, Minnesota 55905 USA

ABSTRACT 1-Sulfonato-8-(1′)anilinonaphthalene (1,8-ANS) was employed as a fluorescent probe of the fatty acid binding site of recombinant rat intestinal fatty acid binding protein (I-FABP). The enhancement of fluorescence upon binding allowed direct determination of binding affinity by fluorescence titration experiments, and measurement of the effects on that affinity of temperature, pH, and ionic strength. Solvent isotope effects were also determined. These data were compared to results from isothermal titration calorimetry. We obtained values for the enthalpy and entropy of this interaction at a variety of temperatures, and hence determined the change in heat capacity of the system consequent upon binding. The ANS–I-FABP is enthalpically driven; above ~14°C it is entropically opposed, but below this temperature the entropy makes a positive contribution to the binding. The changes we observe in both enthalpy and entropy of binding with temperature can be derived from the change in heat capacity upon binding by integration, which demonstrates the internal consistency of our results. Bound ANS is displaced by fatty acids and can itself displace fatty acids bound to I-FABP. The binding site for ANS appears to be inside the solvent-containing cavity observed in the x-ray crystal structure, the same cavity occupied by fatty acid. From the fluorescence spectrum and from an inversion of the Debye-Hueckel formula for the activity coefficients as a function of added salt, we inferred that this cavity is fairly polar in character, which is in keeping with inferences drawn from the x-ray structure. The binding affinity of ANS is considered to be a consequence of both electrostatic and conditional hydrophobic effects. We speculate that the observed change in heat capacity is produced mainly by the displacement of strongly hydrogen-bonded waters from the protein cavity.

INTRODUCTION

Intestinal fatty acid binding protein (I-FABP) belongs to a family of cellular lipid-binding proteins. Several of these proteins have been isolated from various tissues, and they bind fatty acids and other lipids with high affinity (see Banaszak et al., 1994, for a review). However, their precise physiological functions are still unclear. The crystal structures of several (both liganded and unliganded forms) have been solved (Sacchettini et al., 1989; Scapin et al., 1992). The proteins are folded into a single domain with a β-barrel motif, and the ligand is contained within a cavity in the barrel. Comparison of the structures of apo- and holoproteins reveals no substantial conformational differences between the two forms. Twenty-four ordered waters with varying degrees of static disorder (i.e., partial occupancy and high temperature factors) are identified in the apoprotein cavity. Although there appears to be room for ~4 more waters, these are not apparent crystallographically, either because they are disordered or because they are not present. This relatively large amount of water in a pocket designed to bind what are primarily nonpolar molecules is common to this family of proteins but is unusual among proteins in general (see, however, Ernst et al., 1995, for an example of disordered water in a hydrophobic cavity in IL-β1). Thus, natural ligands, namely fatty acids, must insert into a region that is substantially hydrated. Although many hydrogen bond pairs between waters in the cavity and between waters and protein residues in the cavity are suspected from the crystal structure, some of which may be involved either in maintaining the overall protein structure or in positioning groups to interact with the fatty acid (six waters remain in the cavity when fatty acid is bound), in I-FABP there is only one charge in the pocket likely to electrostatically attract and ionically pair with the fatty acid carboxylate, namely arg-106. When arg-106 is replaced by glutamine, I-FABP loses affinity for oleic acid by a factor of about 20 (Jakoby et al., 1993).

The structure of the related fatty acid binding proteins poses an interesting question regarding the driving force(s) responsible for binding of the natural ligand. The commonly held view of hydrophobic interactions is that they are entropically driven (Tanford, 1973; Franks, 1975), so that it is interesting that LaLonde and colleagues (LaLonde et al., 1994) find that fatty acid binding to adipocyte lipid binding protein (ALBP) is apparently enthalpically dominated, seemingly at variance with prevailing wisdom (see, however, Privalov and Gill, 1988; and Dill, 1990, for two views of hydrophobic interaction that stress the role of enthalpic contributions). Thus, from both the result of Jakoby et al. and that of LaLonde et al., there seems to be a role for both electrostatic interactions (here, exothermic) and hydrophobic interactions, possibly related to the liberation of water specifically adsorbed both to I-FABP and to the ligand, which occurs upon I-FABP–ligand association. To evaluate the extent to which one or the other interaction predomi-

Received for publication 30 June 1995 and in final form 11 October 1995.
Address reprint requests to Dr. Franklyn G. Prendergast, Department of Biochemistry and Molecular Biology, Mayo Foundation, 200 First St. SW, Rochester, MN 55905. Tel.: 507-284-2511; Fax: 507-284-9349; E-mail: prendergast@mayo.edu.

0006-3495/96/01/69/15 $2.00

nates we have chosen to use both direct (nuclear magnetic resonance; in a subsequent publication) and indirect experimental approaches.

The fluorescence of (1,8)-anilinonaphthalenesulfonate (1,8-ANS) has been shown to be dramatically sensitive to the presence of H_2O (for a general review, see Slavik, 1982), which has been interpreted in terms of a specific solute-solvent interaction (cf. Fœrster and Rokos, 1967; Dodiuk et al., 1979). There have been other interpretations, however, which have been based on the classical model (cf. Cantor and Schimmel, 1980) of an increased dipole moment of the excited state over the ground state of ANS, leading to increasing redshift with solvent polarity (Weber, 1952; Robinson et al., 1978). However, these latter authors report biexponential fluorescence decay behavior for ANS in ethanol:water mixtures, which becomes resolved into single-exponential behavior in the pure solvents (Robinson et al., 1978), a fact not easily explained by the classical model. Fœrster and Rokos (1967) discovered a large (1.75) D_2O versus H_2O isotope effect on the fluorescence quantum yield in the related system *N,N*-dimethylaminonaphthalene sulfonate, which was attributed to the specific coupling of the nuclear motion of one or more water molecules with the electronic motion of the solute molecule. Both of these studies thus suggest a role for a single water molecule:ANS interaction that stabilizes the excited state, possibly by association, not necessarily because the ANS is more polar in the excited state than in the ground state (because this would result in a simultaneous redshift in absorbance in more polar solvents, contrary to what is observed). This associated water would facilitate quenching of the excited state, possibly by increased electron transfer to solvent (Dodiuk et al., 1979). The linear relationship observed by Robinson et al. (1978) of emission redshift with effective nonradiative decay rate for ANS in ethanol:water mixtures would then be explained by the solvent dependence of the reorganization parameter λ of Marcus's electron transfer theory (Marcus, 1965). This parameter depends on long-range dipolar characteristics of the solvent—λ being larger in more associating, polar solvents. We shall treat the photophysics of ANS in solvent mixtures in a subsequent contribution of our own. For the moment it is apparent that the fluorescence of ANS might provide a useful probe of solvation dynamics in situ in the protein matrix.

ANS has accordingly been used widely as a probe for putative hydrophobic binding sites in proteins and even applied as a diagnostic test for such sites in protein "molten globules" (Sirangelo et al., 1994; Goldberg et al., 1990), the assumption being that ANS binding to proteins is primarily by hydrophobic interactions mediated through its two aromatic moieties. Interestingly, despite its common use for such determinations, proof from x-ray or nuclear magnetic resonance (NMR) structural studies that ANS indeed binds to and reports on hydrophobic sites is lacking, there being only one x-ray structure of bound ANS extant in the literature (Weber et al., 1979). Rather, studies of ANS binding to proteins have generally been limited to evaluations of stoichiometry and binding constants derived from fluorescence titration experiments (e.g., Stryer, 1965) or determinations of quantum yields and fluorescence spectra (cf. Cantor and Schimmel, 1980), the nature of the ligand binding site then being inferred. Judging from the extent of hydration, the binding cavity of I-FABP cannot be considered wholly hydrophobic; at least it is by no means anhydrous in character. Admittedly, there does appear to be a cuff of aromatic residues near the carboxylate binding site in the crystal structure, which apparently induces a kink in the fatty acid chain at C-2,C-3. At least part of the intrinsic binding energy of fatty acid may therefore be utilized to force an unfavorable conformation (compared to solution) upon the alkyl chain as it is bound in the pocket. This entropy cost (cf. Jencks, 1975) could well be less severe in the case of ANS binding, because its aromatic groups have already less configurational entropy than fatty acids.

Given the presumed character of the fatty acid binding pocket in I-FABP and the presumed affinity of ANS for binding to hydrophobic sites, we reasoned that this fluorophore might prove a useful probe of this pocket with a number of possible outcomes. First, the bound ANS might compete with the natural ligand, whereupon the change (presumably a loss) in fluorescence could serve as the basis of an assay for the natural ligand binding. Second, the fluorescence response of ANS upon binding, or of the protein-bound ANS to a variety of physical and chemical perturbations, could provide a valuable probe of the physicochemical characteristics of the binding site.

Our objective in this paper is to evaluate the thermodynamic parameters of the ANS–I-FABP interaction, in an attempt to separate and define the hydrophobic and electrostatic determinants of this interaction. This we have accomplished primarily by using fluorescence measurements and titration calorimetry.

MATERIALS AND METHODS

Protein expression

The *Escherichia coli* strain MG1655 containing the pMON-IFABP vector was kindly provided to us by the laboratory of C. Frieden (Washington University School of Medicine, St. Louis, MO). The vector contains the *rec*A promoter, which is induced with nalidixic acid. *E. coli* cells were grown overnight in 50 ml of 2xYT (cf. Sambrook et al., 1989) medium containing 100 μg/ml ampicillin, and then diluted into 1 liter of 2xYT medium containing 50 μg/ml ampicillin to an OD_{600} of 0.1. The cells were grown in 1-liter shaker flasks to an OD_{600} of 1.0 and then induced with 50 μg/ml of nalidixic acid. The cells were harvested by centrifugation upon reaching an OD_{600} between 6 and 7. About 8 g of cell paste is recovered from 1 liter of culture. The cell paste was kept frozen at −70°C until further use.

Protein purification

Recombinant rat I-FABP was purified from *E. coli* cells containing the pMONIFABP vector by a modification of the method of Xu et al. (1991). Briefly, the frozen cell paste was suspended in the buffer containing 25 mM imidazole, 50 mM NaCl, 1 mM 2-mercaptoethanol, 5 mM EDTA, and 0.1 mM phenylmethylsulfonyl fluoride at pH 7. The cells were lysed using

a French Press cell, rather than by sonication. The solution was spun down, and 5% protamine sulfate solution was added to the supernatant to a final concentration of 1% protamine sulfate. The solution was stirred at 4°C for 20 min and centrifuged. This supernatant was titrated to pH 5.0 with 2 M sodium acetate and allowed to stir 6–8 h at room temperature. The solution was spun again, concentrated, and applied to a G-75 Sephadex column (100 cm × 5 cm) equilibrated with 12.5 mM HEPES, 50 mM NaCl at pH 7.5. The fractions containing I-FABP were pooled, concentrated, and dialyzed against 50 mM Tris-HCl, pH 8.3, and then applied to an anion exchange column (DEAE Sephadex, 5 cm × 1 cm) equilibrated with the same buffer. Pure I-FABP comes off in the void. Purity was assessed by SDS-PAGE; the protein appeared as a single band to Coomassie blue. N-terminal amino acid analysis yielded only one N-terminus. No impurity was detected on a mass spectrum.

Buffer preparations for fluorescence

Morpholinoethane- and propanesulfonic acid and their potassium salts (MES, MES-K.3H_2O, MOPS, and MOPS-K.3H_2O), as well as TES and TES-K, were recrystallized as described (Kirk et al., 1993). HEPES and its sodium salt (HEPES-Na) were obtained from Fluka (Haupaugge, NY). *N*-Cyclohexylaminoethanesulfonic acid (CHES) was obtained from Sigma (St. Louis, MO). The deuterio buffers were prepared from the dry buffer and buffer salts directly for those we recrystallized, whereas those for HEPES and CHES were obtained by lyophilizing the protio buffers and adding the appropriate amount of D_2O. For an ionic strength dependence series, a HEPES buffer stock was prepared, and various volumes of 0.99 M NaCl stock solution were added to obtain buffers with concentrations of 0, 10, 20, 40, 70, and 110 mM added NaCl in 5 mM HEPES.

Fluorescence measurements

Titrations of ANS fluorescence were performed by adding known amounts of I-FABP into buffered solutions containing given concentrations of ANS (ammonium salt, from Fluka, ϵ_{350} = 4990 in H_2O). The entire corrected fluorescence emission spectrum from 390 to 640 nm was collected with a Spex 1680 spectrofluorimeter, and the integrated fluorescence signal over that wavelength region was measured. Most photomultipliers possess a fairly wavelength-neutral region of their response function between 420 and 490 nm (cf. Guilbault, 1973), so that the uncorrected spectrum has the same emission maximum, but the long wavelength tail of the emission is distorted by the PM tube. The concentration of I-FABP in stock solutions was determined by UV absorption spectra (Cary/Varian 2200), using an ϵ_{280} of 18,700/M-cm. This latter value for the protein extinction coefficient differs from a previously published value (16,900; Richieri et al., 1992). Our value is consistent with quantitative amino acid analyses performed in the peptide core facility at this institution and is also more consistent with the titration(s) conducted as described below.

Binding constants are extracted from fluorescence titration data from the analysis of δf, which is a normalized fluorescence difference function due to enhancement of ANS fluorescence upon binding to the protein and is developed in terms of the fluorescence (F) of a solution in the presence of a given amount of protein (P) and ANS (A), called $F(P, A)$ thus:

$$\mathcal{F}(P, A) = \mathcal{F}(0, 0) + (1 - x)q_A A + x\phi q_A A \qquad (1a)$$

$$\mathcal{F}(0, A) = \mathcal{F}(0, 0) + q_A A. \qquad (1b)$$

The rationale for this formalism is as follows. We model the fluorescence actually obtained at a given concentration P and A as the sum of 1) a background fluorescence (that obtained in the absence of protein and ANS), $F(0, 0)$, due mostly to scattering from stray light; 2) the fluorescence due to unbound ANS, which is the fluorescence that would be obtained from the same concentration of ANS without protein and is directly proportional to the concentration of A times a term proportional to its quantum yield, q_A, multiplied by $1 - x$, where x is the fraction of ANS bound to I-FABP; and 3) the fluorescence due to bound ANS, which is proportional to the fraction of ANS bound, the fluorescence of ANS at its given concentration (i.e., $q_A A$), and an enhancement factor ϕ, which measures the increase of fluorescence of bound over free ANS. The above formalism assumes linear relationships between the fluorescence of bound ANS and its concentration, and the fluorescence of free ANS and *its* concentration. Because the number of photons observed is proportional to the number of fluorophores of a given kind that are excited and observable in the emission light path and hence, for any series of measurements, to the concentration of the fluorophore as long as this concentration is small and inner filter effects can be ignored, this assumption is usually justified (cf. Guilbault, 1973, also: Cantor and Schimmel, 1980). At 2.5 μM the extinction of the ANS at 330 nm is 0.0075, so the inner filter effect correction was not calculated (Brand and Witholt, 1967). Because of the normalization we employ, the exact value of q is not necessary for our further analysis here; merely the linearity of fluorescence with fluorophore concentration is assumed. We have further established the validity of these assumptions over our experimental concentration regime (cf. Kurian et al., submitted for publication). Constructing now the difference function δf:

$$\delta f = \{\mathcal{F}(P, A) - \mathcal{F}(0, A)\}/\{\mathcal{F}(0, A) - \mathcal{F}(0, 0)\}, \qquad (1c)$$

we find it to be equal to $(\phi - 1)x$ from the Eqs. 1a and 1b. Thus we find x in terms of observables and one parameter, ϕ. If a 1:1 binding stoichiometry is assumed, then

$$K_d = (1 - x)(P - Ax)/x. \qquad (2a)$$

We can now isolate the variable (concentration of added I-FABP, or P) and fixed and to-be-fitted parameters (A, K_d, and ϕ) on one side of the equation, and the observable (δf) on the other, by solving for x in the resulting quadratic in terms of the dependent and independent variables:

$$\delta f = \frac{P + A + K_d - [(P + A + K_d)^2 - 4AP]^{1/2}}{2A/(\phi - 1)}. \qquad (2b)$$

At this point, a nonlinear least-squares routine can be employed (as is provided in KaleidaGraph—Abelbeck Software; similar to what was attempted, for example, by Yang et al., 1994) to extract values for K_d (in molarity) and ϕ. However, it should be noted that values of ϕ and K_d are positively correlated, i.e., the larger the trial value of K_d assumed, the larger ϕ must become to accommodate the data, and vice versa, leading to runaway solutions when there is appreciable error in δf at low concentrations, as was often the case, if a poor choice of trial values is made. A more robust procedure is to include a parameter that corrects for concentration variation between identical runs, because our data were run in triplicate (Brandts, 1993). This parameter can appear as a factor of the variable concentration P or else on the fixed concentration A. We have chosen the former to minimize the number of times it must be employed in the fitting equation. It should also be pointed out that the additions of I-FABP to ANS in buffer that we made in no case exceeded 3.5% of the original volume, so we made no concentration corrections to the data. Nonetheless, by this factor alone the concentration of ANS in the sample is not constant within a single titration run, regardless of slight variations due to pipetting errors from run to run. The following quadratic was employed instead, which, as we observed, indeed recovered K_d and ϕ values with less sensitivity to their initial input parameters:

$$\delta f = \frac{nP + A + K_d - [(nP - A + K_d)^2 + 4AK_d]^{1/2}}{2A/(\phi - 1)}, \qquad (2c)$$

where n is the correction factor discussed above. Values for n were in all cases close to 1.00, as we expected, but the allowed error in n helped to fit the distribution of the data, because it acts as another degree of freedom. Fitting the same quadratic without using the n parameter gave very similar results, but with a larger value for χ^2. Significantly, the mentioned correlation above between what are a priori independent parameters, ϕ and K_d, is diminished with the use of this parameter. (The correlation noted above between K_d and ϕ is apparent from comparison of the fittings obtained

from Eqs. 2b and 2c. If one of the fittings has a larger value of K_d than the other, then it also has a larger value of $\phi - 1$. Generally n is found to be less than 1, and the values of both K_d and $\phi - 1$ for the fitting with n as a degree of freedom are both smaller. This correlation can be expressed in terms of a correlation coefficient and the expressions 2b and 2c compared by the degree to which this correlation becomes less significant. These coefficients are given as a function of the added protein concentrations P_i by

$$\mathrm{c(2b)} = \frac{\sum_j (\delta f_j/(\phi - 1) - 1)(K/2A)(1 - (P_i + A + K)}{((P_i + K + A)^2 - 4AP_i)^{1/2}};$$

over j identical observations, and

$$\mathrm{c(2c)} = \frac{\sum_j (\delta f_j/(\phi - 1) - 1)(K/2A)(1 - (nP_i + A + K)}{((nP_i + K + A)^2 + 4AK)^{1/2}};$$

Typical results for lower values of P_i are ~0.35 for c(2b) and ~0.3 for c(2c), whereas at the highest values of P_i c(2b) $\approx$ 0.04 and c(2c) $\approx$ 0.03.) Although it would have been feasible to extract these binding constants from other kinds of data analysis (e.g., Scatchard plots), these traditional methods are open to various objections (cf. Klotz, 1982). The most significant criticism of such methods is probably that the data as transformed by these methods are not equally weighted in terms of their errors, and hence neither the standard linear nor nonlinear regression method is robust for these data sets (Cornish-Bowden, 1995). The standard methods can themselves be adapted to transform the errors to an equally-weighted format, but this requires a significant amount of extra programming. Our method can utilize the nonlinear least-squares routine offered in commercially available software. These transforming methods were originally devised as graphical methods to circumvent the need for data analysis by computer; the speed and ready availability of modern personal computers has rendered this issue largely moot.

Fluorescence lifetimes for ANS in H_2O, D_2O, and on I-FABP in H_2O and D_2O buffers were determined by use of time-correlated, single photon counting (cf. O'Connor and Ware, 1976), with excitation at 295 nm, and emission monitored at 490 nm, as well as by a multifrequency phase and modulation apparatus (as described in Kirk et al., 1993).

Quantum yields were obtained by comparison of total fluorescence against that of quinine bisulfate (recrystallized from 90% ethanol:water and dried overnight at 50°C in a dessicator) in 2 N H_2SO_4 (quantum yield 0.55 at 23°C; Demas and Crosby, 1971) as a standard. Calculated values for the radiative rate constant were obtained from the absorption spectrum and the normalized fluorescence spectrum, via the relation (cf. Strickler and Berg, 1962):

$$k_{rad}(s^{-1}) = 2.8809 \times 10^{12} n^2 \int \epsilon(\nu)/\nu \, d\nu \Big/ \int f(\lambda)\lambda^3 \, d\lambda, \quad (3)$$

where $f(\lambda)$ is the normalized fluorescence spectrum for λ in nanometers, $\epsilon(\nu)$ is the molar absorptivity as a function of frequency (ν) in cm^{-1}. We employed index of refraction (n^2) corrections throughout, using a Zeiss refractometer to measure n.

Calorimetry

Isothermal titration calorimetry was performed using a MicroCal (Norhthampton, MA) calorimeter. Typically, 4 μl of 2 mM ANS at a time was injected into 1.53 ml of 0.0545 mM FABP, and the excess heat per second was measured (as feedback power to a differential amplifier) as a function of time after each injection, until thermal equilibrium with a reference cell was reestablished (~400 s). The integral of these data, when normalized for concentration, and after a control titration of ANS into buffer had been subtracted, yields a binding isotherm of heat (per mole) produced per injection versus concentration of added ligand (cf. Fig. 4 *c*), from which ΔH for the binding process is determined and K_d values extracted. The data from the first injection are ignored (although the added ligand concentration is accounted for), because there is a modest amount of ligand from the stirrer tip before and during preequilibration. The calorimeter is calibrated by comparing the integral heat of pulses from an internal heating circuit with the expected heats from Ohm's law. The variance for several calibration runs was ~0.3% from the manufacturer-supplied calibration constants.

ΔH for binding can essentially be read off as the total vertical distance between the beginning and the end of a titration for this binding isotherm (assuming that the titration does go to completion), as in Fig. 4 *c*, for example. This is then the ΔH of the binding process, regardless of what K_d turns out to be (again, assuming that the titration is complete). The value for K_d is determined by a nonlinear least-squares routine very similar to the one introduced above by fitting

$$Q_i = \frac{\Delta H V_0}{2[nM + L_i + K_d - ((nM + L_i + K_d)^2 - 4nML_i)^{1/2}]} \quad (4)$$

where Q_i is the heat evolved in the ith injection, V_0 is the (known) volume of the ITC cell, M is the concentration of macromolecule, and L_i is the concentration of added ligand at the ith injection.

RESULTS

Fig. 1) shows typical results for the fluorescence titrations. There is substantial enhancement of the fluorescence of ANS upon increasing protein concentration (Fig. 1 *a*). The fluorescence emission is also shifted to the blue (from ~545 to ~480 nm). Both these results are in a range typical of the binding of this ligand to other proteins (see Slavik, 1981). Analysis of the raw binding data as described above is presented as a plot of δf versus the concentration of added I-FABP as discussed in Materials and Methods, as in Fig. 1 *b*). It is from plots such as these that we first extract apparent dissociation constant K_d and enhancement factor ϕ values. These results are similar to what is seen for the binding of 2,6-ANS, a positional isomer of 1,8-ANS. For 2,6-ANS there is also a blueshift and an enhancement of fluorescence upon binding (~40-fold). But the binding of 2,6-ANS to I-FABP is a factor ~65 weaker than that for 1,8-ANS (data not shown). To characterize the thermodynamics of the binding of 1,8-ANS more fully, we performed a series of titrations at a variety of temperatures for a van't Hoff analysis, our intention being to obtain values of ΔH and ΔS of 1,8-ANS binding to I-FABP (see Table 1 and Fig. 2). The enthalpy obtained from the slope of the plot in Fig. 2 is −6.5 kcal/mol. This result implies that the binding event is in fact enthalpically driven, given that the value of ΔG is ~ −6.8 kcal/mol, regardless of temperature (cf. Table 2).

Fig. 3 displays results obtained at 22°C with titration calorimetry. We present both the raw data (Fig. 3 *a*) and the normalized integral of these data (Fig. 3 *b*). The calorimetrically derived values for the ΔH of binding (obtained from fitting normalized integral data such as in Fig. 3 *b* for the various titrations, as we discussed in Materials and Methods) at various temperatures are shown in Fig. 4. The slope of the linear region is approximately −283 cal/deg-mol. The calorimetric values for ΔH span a range that includes the van't Hoff value of −6.8 kcal/mol, but the values do not coincide at 22°C (the midpoint of the van't Hoff data), the

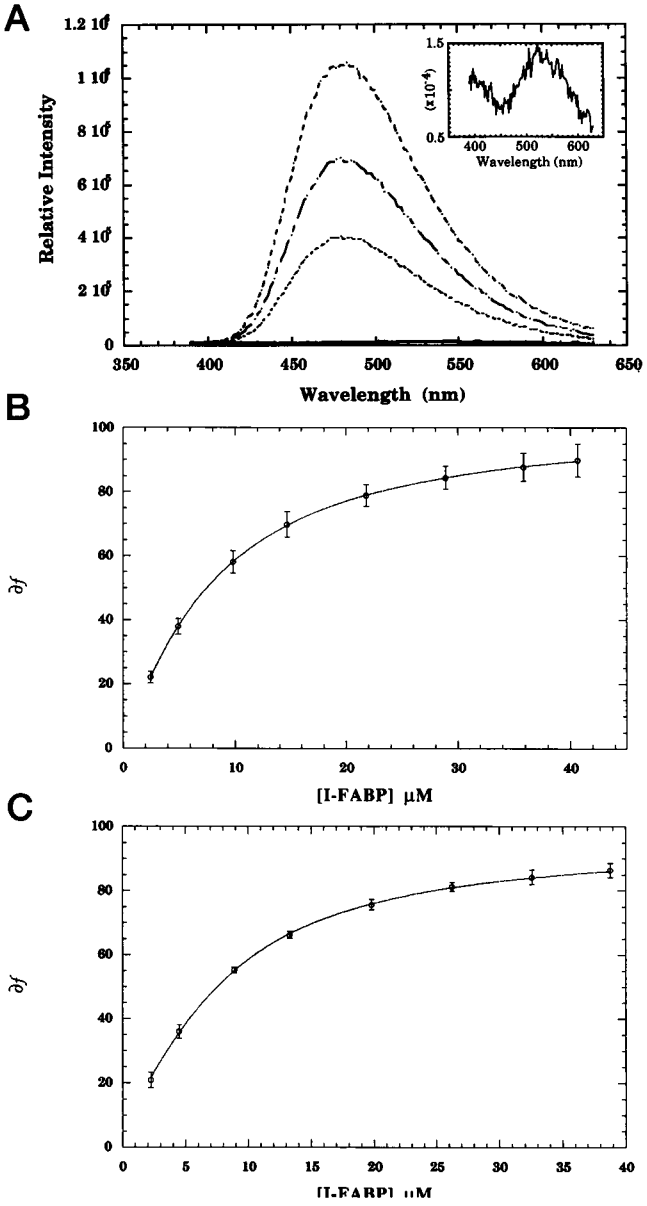

FIGURE 1 (*a*) Spectra recording part of the titration of I-FABP into 2.725 μM ANS in HEPES/Na 0.05 M, with 0.05 M NaCl, pH 7.53. I-FABP stock was 1.01 mM. This titration was performed at 15.8°C. ——, ANS in buffer, no addition; rescaled 20× in inset; ···, addition of 5 μl I-FABP, [I-FABP] = 2.35 μM; — - —, [I-FABP] = 4.7 μM; - - -, [I-FABP] = 9.3 μM. (*b*) Results of the experiment in *a*, plotted as the normalized difference function δf described in the text, versus [I-FABP]. The curve displayed is the result of the fitting procedure, as described in the text. (*c*) Same conditions as in *a*, except that T = 18.6°C. Results of fitting procedure are also given in Table 1. All runs are in triplicate; error bars shown are standard deviations.

most likely place for the direct and the van't Hoff enthalpy to coincide. There is also no indication of curvature in the van't Hoff plot, despite the large change in enthalpy observed calorimetrically over the temperature range 5–37°C.

Because of the large fluorescence enhancement factor, we can generate our fluorescence titration data using a protein-concentration regime that encompasses the actual K_d (from

TABLE 1 Binding parameters as a function of temperature*

Temperature (°C)	K_d (μM)	ϕ	n
4.7	4.6 ± 3.3	130 ± 19	0.92 ± 0.60
7.7	4.8 ± 1.4	112 ± 6	0.92 ± 0.20
10.2	5.2 ± 1.6	110 ± 6	0.95 ± 0.18
13.0	6.8 ± 1.6	111 ± 6	1.00 ± 0.04
15.8	6.7 ± 1.9	111 ± 5	0.97 ± 0.08
18.6	6.9 ± 1.0	105 ± 4	0.98 ± 0.08
21.5	8.8 ± 1.2	105 ± 2	0.99 ± 0.03
24.5	9.7 ± 4.0	99 ± 7	1.03 ± 0.05
27.3	9.8 ± 2.8	114 ± 7	0.99 ± 0.04
30.5	11.4 ± 1.0	106 ± 2	1.00 ± 0.01
33.4	12.8 ± 2.1	98 ± 5	1.00 ± 0.01
36.4	15.9 ± 3.2	94 ± 5	1.00 ± 0.01

*Parameters as described in the text, obtained by fitting Eq. 2 to data as in Fig. 1, *a,b*. Standard errors are given.

roughly 0.5× to ~5× K_d), whereas the ANS concentration is on the order of K_d. This implies that the response in fluorescence signal to increments in protein concentration is optimal, while maintaining a useful amount of curvature in the plot of δf versus [I-FABP]. (The curvature is determined by the remainder inside the surd of Eq. 2c, i.e., $4AK$, without which the plot would be a straight line, so that the points where there is considerable curvature essentially determine the fitted parameters. This can be seen by imagining a titration occurring over a range of protein and ANS concentration ~100 times K_d versus 1000 or 10,000 times K_d. In both cases a straight line is observed until [I-FABP] equals [ANS], and there would be no distinction between the two cases in the appearance of the titration data. Therefore the the best that could be obtained would be an upper limit to K_d. Similarly, at concentrations of ANS $\ll K_d$, the titration data are indeed curved, but δf is now such a slowly varying function of [I-FABP] that it seems to be a straight line.) Furthermore, at low protein concentrations, the function in Eq. 2 has greater sensitivity to small variations in the fitted parameter values of K_d, than at higher concentrations; hence we expect the fluorimetric ΔG values to be more accurate than the K_d from calorimetry, which, although

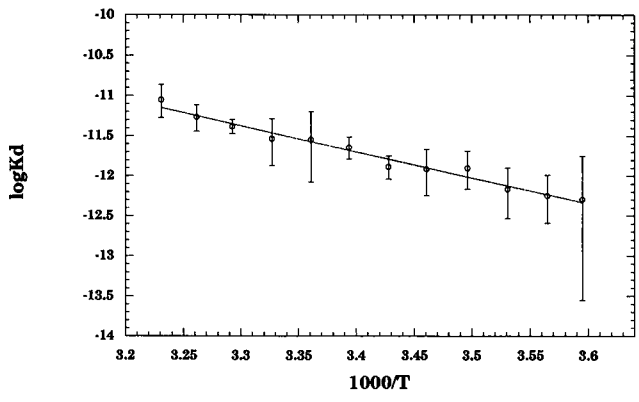

FIGURE 2 Data as shown in Table 1, replotted as ln K_d versus $1000/T$ (temperature in Kelvins). Best slope is ~ −3.25, which multiplied by R gives the van't Hoff value for ΔH (~6.45 kcal/mol).

TABLE 2 Thermodynamic parameters for ANS-IFABP binding

	Direct titration		Calorimetry		Best value†
	$\Delta G°$ (kcal/mol)	$\Delta H°$ (kcal/mol)	$\Delta G°$	$\Delta H°$	$\Delta S°$ (cal/deg-mol)
pH 7.53 HEPES*					
8°C	−6.8	van't Hoff	−6.7	−4.4	+8.5
22°C	−6.8		−6.9	−8.6	−6.1
		−6.5 ± 1.8			
30°C	−6.85		−7.1	−10.5	−12.0
36°C	−6.8		−6.8	−10.6	−12.3
pH 8.84 CHES§					
5.6°C	−6.3		−6.2	−8.7	−8.6
22°C	−5.3		−5.8	−11.8	−22.0

*The HEPES was made 1:1 zwitterion:conjugate base ratio. At 25°C, this corresponds to pH 7.53 with a ΔpK/°C of −0.017. The composition was 0.0675 M, with 50 mM NaCl.

†The "best value" is obtained using the fluorescence titration $\Delta G°$ and the calorimetric $\Delta H°$.

§CHES buffer was 0.0675 M, 50 mM NaCl.

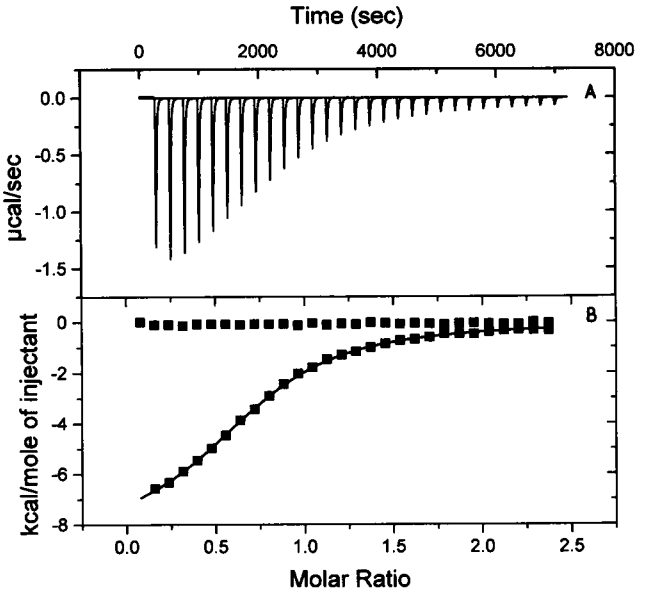

FIGURE 3 Isothermal titration calorimetry (ITC) experiment at 22°C. ANS (2.1 mM) was added to 54.5 μM I-FABP in HEPES buffer at pH 7.53 as described in the text. (*A*) The raw titration data; (*B*) the integral of these data, normalized to the protein concentration. The fitting (fitted curve is also shown) results in a value for the association constant of 1.2 ± 0.032 × 10^5/M, and a ΔH of −8630 ± 92 cal/mol.

derived from a fitting similar to the methodology employed for the fluorescence titration K_d, is unavoidably obtained in a concentration regime ~10–20 × K_d. This latter range of concentrations is chosen to obtain the best results from microcalorimetry (best heat signal), but it may not, for the reason stated, yield the best data for fitting K_d. However, the directly measured value of ΔH from calorimery should be more accurate than the van't Hoff enthalpy, because that enthalpy is only found from the average slope over the whole set of temperatures. In Table 2, we present the best value for ΔS at three temperatures: $\Delta S_{best} = (\Delta H_{calorimetry} - \Delta G_{fluorescence})/T$ at each temperature T.

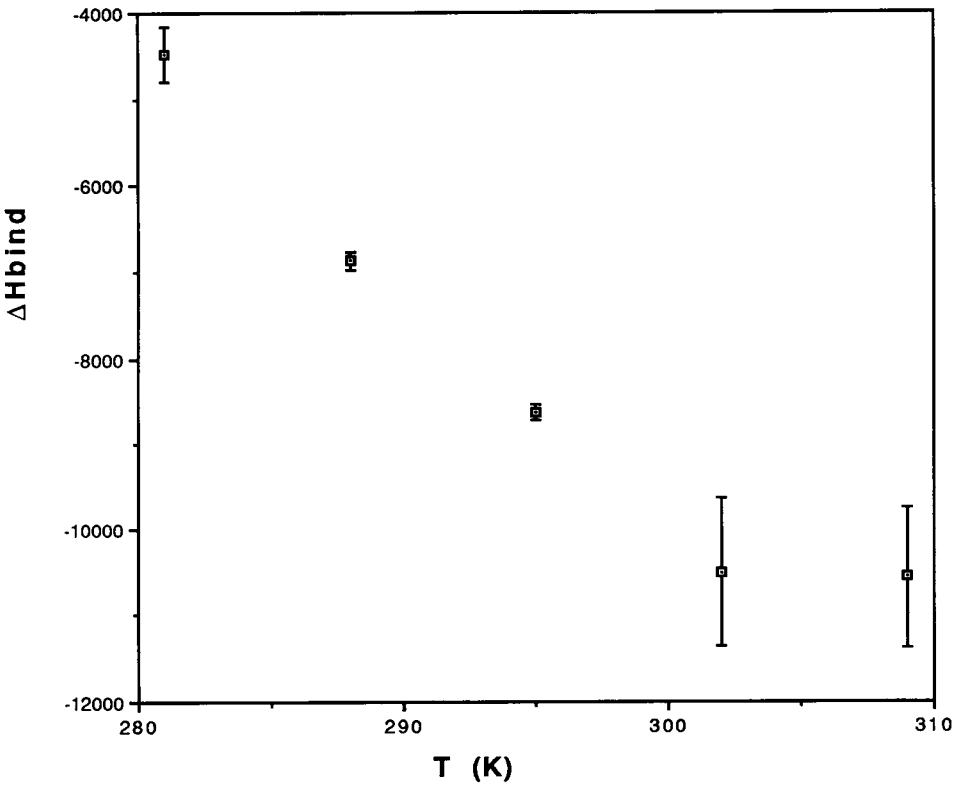

FIGURE 4 ITC values for ΔH of binding at various temperatures. Error bars are the standard error of the fitted parameter. The injection syringe jacket was not temperature-controlled in the space above the calorimeter access port; thus at observation temperatures very different from room temperature the data were noisier, which contributes to the observed errors.

In Fig. 5, we plot the values of K_d obtained by our fluorescence titrations at various pHs (pDs) in H_2O or D_2O. The affinity of the protein for ANS falls off at higher pH. The simplest explanation for this would be a deprotonation event on the protein. The most likely candidate for a deprotonation event directly affecting the affinity would be arg-106, but the pH value observed (~8.9) is too low for a typical argininyl residue to deprotonate. A lys or his residue would seem more appropriate; there appear not to be any other obvious candidates in the binding cavity. Interestingly, the emission of bound ANS shifts slightly to the red (from 481 to 478 nm) at this pH. The most we can point out from the data in Table 2 is that going from neutrality to pH 8.9 causes the binding event to become 3.2 kcal/mol more enthalpically driven, but ~ 4.7 kcal/mol more entropically opposed, i.e., the change in enthalpy and entropy are of the same (negative) sign.

A purely electrostatic origin of these changes at high pH is not impossible, because $\Delta S_{el} = -\Delta G_{el}/\epsilon \, d\epsilon/dT$, and $d\epsilon/dT < 0$. If we compare the affinities at the same relative position on the pH/pD scale, i.e., within the maximum region, or at a minimum, we see that the isotope effect is a remarkably constant ~3, favoring D_2O. The isotope effect on binding may then be taken to be essentially independent of this particular electrostatic contribution, although it may, and probably does, depend on the existence of a charge on the ANS, which does not change its ionization state throughout the entire pH/pD range.

Assuming that an electrostatic interaction between the sulfonate and some moiety on the protein is significant, we chose to evaluate further the possible contribution of electrostatic forces to the binding affinity, by studying the effect of added salt on the K_d. If we suppose that the major electrostatic contribution arises from the interaction of a univalent cation with a univalent anion (as, for example, ANS and arg-106 of I-FABP), then the actual K_d at a given ionic strength, or $K_d(I)$, may depend on a limiting (standard) value of K_d ($K_d(0)$) and an activity coefficient correction for both charged species $\gamma_{\pm}$, as well as the uncharged complex $\gamma_{complex}$. Thus:

$$\log K_d(I) \equiv \log\left(\frac{[+][-]\gamma_{\pm}^2}{[\text{complex}]\gamma_{\text{complex}}}\right) = \log K_d(0) + \frac{\log \gamma_{\pm}^2}{\gamma_{\text{complex}}} \tag{5}$$

If any specific residue of I-FABP interacts with the sulfonate anion of ANS, then it must also be univalent (there being no multivalent amino acid residues). For a 1:1 charge: charge interaction, the $\gamma_{complex}$ should not be a critical function of the ionic strength I.The reason for this is that the ion pair, or the zwitterion, so formed behaves like a dipole, which, to first order, does not attract an ionic cloud within the solvent medium about itself as a bare charge would (Kirkwood, 1934). But we should expect $\gamma_{\pm}$ to vary according to the Debye-Hueckel limiting law, namely:

$$\log \gamma_{\pm} = -|z_+ z_-| \, (1/4.606)(e_0^2/\epsilon k_B T)^{3/2}(8\pi N_A/1000)^{1/2}(I)^{1/2} \equiv \Gamma(I)^{1/2} \tag{6}$$

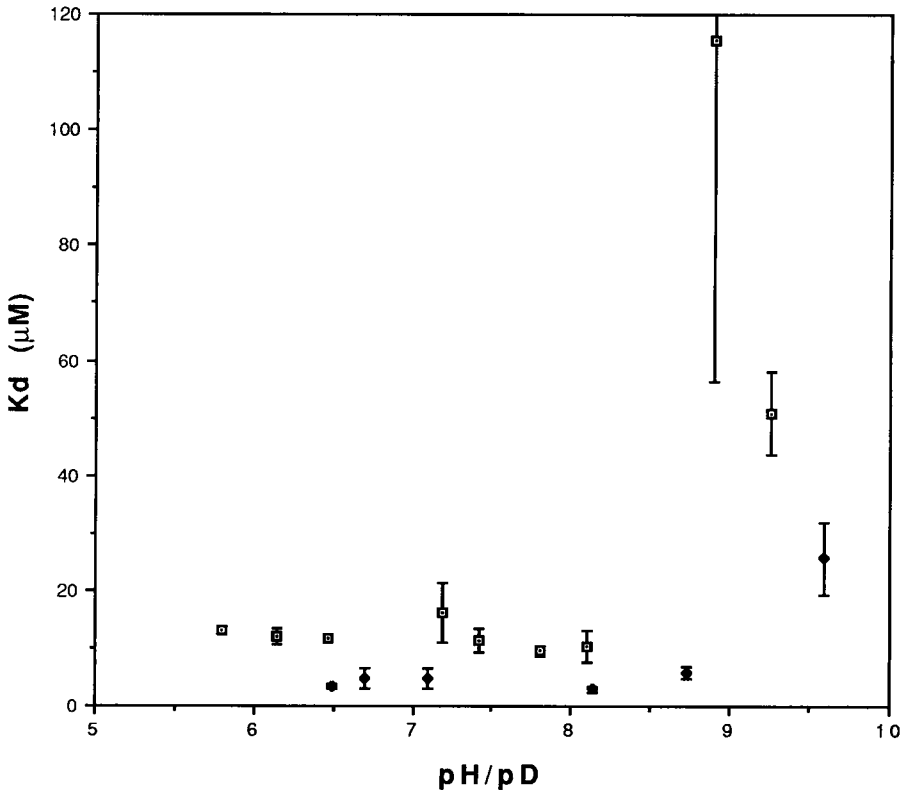

FIGURE 5 The dependence of K_d on pH (q) or pD (u). The errors shown are standard errors to the fit of fluorescence titration experiments. In the case of pH 8.84, the experimental protocol (similar to that employed in other experiments; cf. Fig. 1) titrates I-FABP into ANS only up to ~⅓ of K_d, which explains the large uncertainty. The data point at pH 9.3 is obtained with a different protocol, allowing the ANS to be titrated to 95 μM concentration, and hence has a smaller standard error. The buffers employed were all 0.0675 M, with 50 mM added NaCl. For pH 5.85, 6.15: MES-H/K was employed; for pH 6.5, 7.18: MOPS-K/H; for pH 7.42, 7.81, and 8.1: TES-K/H; for pH 8.84, 9.3: CHES-Na/H. For pD 6.47, 6.71: MES-K/D was employed; for 7.1: MOPS-K/D; for 8.17, 8.71: TES-K/D; for pD 9.6: CHES-Na/D.

for relatively low ionic strengths. In Eq. 6, k_B is the Boltzmann constant, N_A Avogadro's number, e_0 the charge on the electron, and e the dielectric constant. For pure water at 22°C, the coefficient of the $\sqrt{I}$ term, Γ, in Eq. 6 is ~0.51 (Bockris and Reddy, 1977). Thus the slope of log $K_d(I)$ versus $\sqrt{I}$ should be ~1.02 for a 1:1 charge interaction in water. The data in Fig. 6 demonstrate what we observed. The best value for the slope is actually 2.6 ± 0.5.

The fluorescence lifetime of ANS in the I-FABP-ANS complex in H_2O is 20.4 ns, and in D_2O is 25.9 ns (HEPES 0.05 M, with 50 mM NaCl), whereas the corresponding lifetimes of free ANS in H- and D-containing buffered solutions were 0.27 and 0.67 ns, respectively (see Fig. 7). The quantum yields for ANS in H_2O and D_2O are 0.0025 and 0.0054, respectively, whereas that for I-FABP (H_2O)-bound ANS is 0.89. The observed radiative rate constant for ANS in water (i.e., quantum yield/lifetime) is thus 9.3×10^6 s^{-1}, whereas the calculated k_{rad} (via Eq. 3) was 2.4×10^7 s^{-1} (the discrepancy between the observed and calculated values of k_{rad} is even worse for D_2O, k_{rad} observed being ~8.1×10^6 s^{-1}). For ANS bound to I-FABP, the observed k_{rad} was 4.4×10^7 s^{-1} versus our calculated value of 4.6×10^7 s^{-1}. Hence, there is a discrepancy to be explained in the pure buffer case, which does not exist in the case of protein-bound ANS, essentially an anomalously long radiative lifetime in water, which may be an indication of at least partial isolation from radiative pathways of the excited state as it exists in buffered aqueous solution (Douglas, 1966). Furthermore, the ratio of lifetimes does not equal the ratio of quantum yields in H_2O and D_2O, which suggests an isotope effect on k_{rad}. There is probably a small error in the quantum yield values, at least for the value of ANS(H_2O) bound to I-FABP of 0.89, because, given the steady-state fluorescence intensity ratio in D_2O versus H_2O for I-FABP bound-ANS fluorescence (1.14; data not shown), the quantum yield in D_2O would then have to be 1.01 (i.e., 1.14 × 0.89).

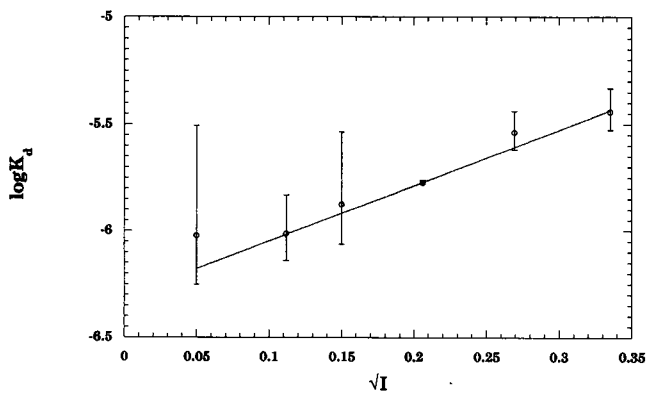

FIGURE 6 Decimal logarithm of K_d versus square root of ionic strength for various additions of NaCl to 5 mM HEPES-Na buffer, pH 7.5. The decimal logarithm is used here, rather than the natural logarithm, because the coefficient in the Debye-Hueckel formula for $\log_{10} \gamma_{\pm}$ in water is thus 0.51 at 22°C (see text). Best-fit line is shown.

Inspection of Figs. 5 and 6, and comparison with Table 1, will show that the values of K_d observed in Fig. 6 are much lower than in Figs. 5 or 1 (or in the table), whereas in general the values in Table 1 are smaller than those in Fig. 5. It is evident in fact that K_d in HEPES buffer at 50 mM salt is much lower than at a very similar pH and 50 mM salt in TES buffer (~40%), whereas the values in 5 mM HEPES are ~4 times smaller. This observation implies that the sulfonate buffers are competing for the binding to I-FABP with ANS. Because one expects the apparent $K_{d,\,app}$ to vary as $K_{d,\,app} = K_{d,\,int}(1 + B/K_{buff})$, where $K_{d,\,int}$ is the intrinsic dissociation constant of ANS, B is the buffer concentration, and K_{buff} is the dissociation constant for the buffer binding to I-FABP, then HEPES has a $K_{buff} \approx 15$ mM, and the K_{buff} for TES and MOPS are roughly 10 mM each. We believe these complications, although a nuisance, do not compromise the conclusions one obtains in our analyses within each series of experiments, because the buffers are always the same or are varied in a systematic way. For example, the data of Fig. 6 are obtained with 5 mM HEPES and no added salt. The K_d under these conditions is 1.0 ± 0.5 μM. When 5 mM Tris buffer (which is not anionic, as are the sulfonate buffers) is employed with no salt, the K_d is 1.6 ± 0.4 μM, which is identical to the K_d in HEPES within experimental error. To be more quantitative, we can write what one expects with the buffer effect as a function of the ionic strength:

$$\log K_d = \log K^0_{d,int} + \log \gamma^2_{\pm} + \log(1 + B/K^0_{buff}\gamma_+) \quad (7a)$$

where $K^0_{d,\,int}$ and K^0_{buff} are the limiting values for K_{int} and K_{buff} as the ionic strength approaches zero. The final term can be expanded as a function of I, whence, keeping only the linear term, because $B/K_{buff} < 1$ at 5 mM B:

$$\log K_d = \log K^0_{d,int} + \log(1 + B/K^0_{buff}) + \Gamma(2 - B \ln 10/(2\gamma(K^0_{buff} + B)))(I)^{1/2} \quad (7b)$$

With B = 5 mM as in Fig. 6, and K^0_{buff} = 15 mM, then the slope of a plot of log K_d versus $I^{1/2}$ is now $\Gamma(2 - 0.26)(I)^{1/2}$ (for $\gamma_{\pm} = 1.1$), instead of $2\Gamma(I)^{1/2}$, as we had supposed, and so the above coefficient for the expected slope of Eq. 6 is not 1.02 $|z_+z_-|$, but 0.89$|z_+z_-|$.

For Fig. 5, where, of necessity, a variety of buffers are employed, one can imagine that the results are only qualitatively correct as regards the broad, fairly flat range of pH corresponding to the minimum of K_d. That is, from one pH to another in this range, the small variations one sees are possibly attributable to this buffer effect alone. However, at the high pHs, the quantitative change in K_d is so large that any secular variations due to differing buffer affinity should be very small, implying that the comparisons we have made of $\Delta G°$ and $\Delta H°$ at this pH versus lower pHs (as in Table 2) should remain valid. To test whether the changes at high pH can be at all attributable to a buffer effect, we have conducted a calorimetric titration of CHES buffer at pH 8.9 into 0.4 mM I-FABP buffered with 50 mM Tris at pH 8.9. The ITC data are shown in Fig. 8. The total heat is very small and practically indistinguishable from that involved in the simple dilution of CHES

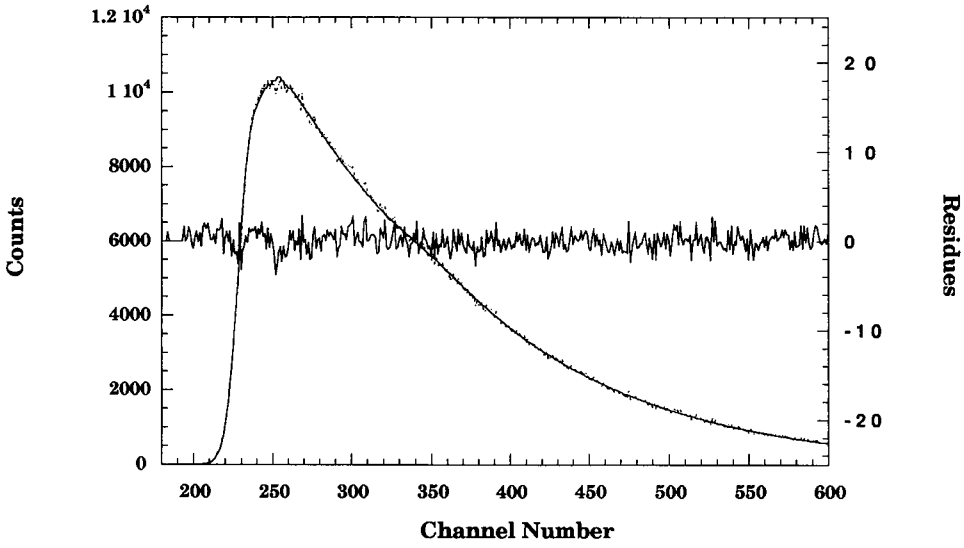

FIGURE 7 Single-photon counting decay observed for 20 μM 1.8 ANS in HEPES buffer, pH 7.5 (5 mM, 0 NaCl). Excitation at 340 nm (with polarizer set at the magic angle before the sample), emission monitored at 520 nm, with 5-nm-wide emission monochrometer slit and 2.569 ps/channel. The recovered lifetime here was 0.268 ns (with a small component at 0.015 ns), $\chi^2 = 1.23$. Residuals are shown superimposed on the data.

buffer in the absence of I-FABP (the best-fit enthalpy of the reaction is roughly -0.15 kcal/mol). If the quantitative differences seen at high pH were due entirely to a buffer effect, then CHES would have to possess a K_{buff} of 1–2 mM, which would have been easily measurable by this experiment. If the effect of pH were due instead to the titration of, e.g., arg-106, then presumably the change in K_d for ANS is due to a change in $K_{d,\ int}$. Then the value of K_{buff} should also be ~10 times the value of K_{buff} at neutral pHs, or in other words ~100 mM, for the same cause as in $K_{d,\ int}$ for ANS. It would be then difficult to detect binding of CHES to I-FABP in our experiment, which indeed is the result.

DISCUSSION

The substantial enhancement of the fluorescence intensity as well as the blueshift of the emission in the presence of I-FABP, together with the results of titration calorimetry, all indicate binding of ANS to the protein. Moreover, bound fatty acid is displaceable by ANS, and vice versa (data not shown). The effective stoichiometry of ANS–I-FABP binding is 1:1 (Kurian et al., submitted for publication). The ANS–I-FABP complex thus provides the basis for a simple competitive assay for fatty acid binding to I-FABP and related proteins in this family (as discussed by Kirk et al., 1995) and indeed is likely to serve as a model assay for other lipid-binding proteins in the same family. The focus of this discussion, however, will be to interpret the fluorescence and calorimetry data in terms of a physical model of the fluorophore-protein complex.

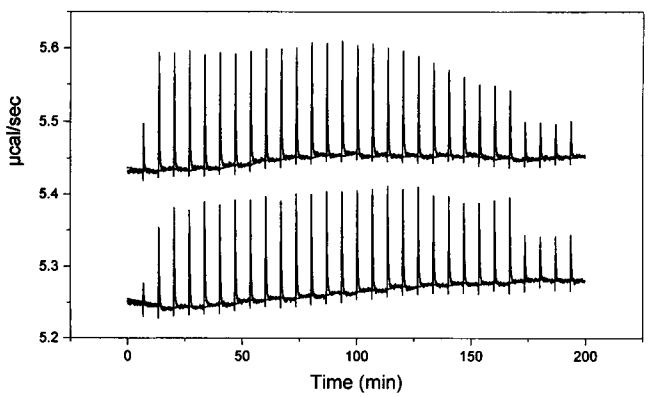

FIGURE 8 Titration calorimetry experiment to test the buffer effect for CHES. (*Lower curve*) 20 mM CHES in 50 mM Tris/Cl buffer, pH 8.9, was titrated in 4-μl increments into 1.535 ml of I-FABP (0.4 mM) dissolved in 50 mM Tris/Cl buffer at 22°C (the first addition is only 2 μl). Four hundred seconds elapsed between injections. (*Upper curve*) CHES-containing buffer is titrated into buffer alone. The CHES was prepared to pH 8.9 before addition of the Tris/Cl buffer. The upper curve has been arbitrarily displaced upward by 0.15 μcal/s to display the whole data set.

Without knowing precisely where ANS binds in the I-FABP structure, or the conformation of the bound ANS, precise interpretation of the molecular basis for the fluorescence enhancement is not yet possible. However, because ANS competes with fatty acid binding, and knowing how the fatty acid binds (i.e., palmitate; Sacchettini et al., 1989), one can reasonably speculate that ANS resides somewhere in the fatty acid binding pocket.

We propose that the sulfonate of ANS corresponds to the carboxylate of fatty acid, and the aromatic moiety is nonpolar and might effectively resemble the alkyl chain of the the fatty acid. The x-ray crystallographic structure of I-FABP with bound palmitate shows that the fatty acid carboxylate interacts with the guanidinium moiety of arg-106 in the binding pocket. Toward the solution face from the deeply buried arg-106-palmitate carboxylate (C-1) binding site, there appears a "kink" in the fatty acid chain (C-2 to C-4). Accordingly, substantial steric constraints, particularly with the rigid naphthyl ring, might prevent the full electrostatic energy of binding the sulfonate to the arg-106 guanidino group from being realized, by preventing the same near approach of sulfonate-to-guanidino moiety that is presumably allowed for the carboxylate-to-guanidino structure. Aromatic residues near the carboxylate binding site that may be responsible for introducing the "kink" in bound

fatty acid, could, on the other hand, interact better with ANS than with fatty acid. The frequencies and amplitude of ring vibrations are usually very similar for naphthyl, indole, and phenyl rings, but are very different from those for skeletal vibrations of alkyl chains; hence London forces between two aromatics or between two aliphatics are stronger than between aromatics and aliphatics (cf. Nemethy and Scheraga, 1962; also Okubo and Ise, 1969).

However, inevitably the actual mode of binding utilized by ANS probably differs, at least in some respects, from that utilized by fatty acid. It is possible, for example, that trp-82 is differently situated in the ANS complex than in the crystal structure, and thus that it might be an interaction site for one of the aromatic moieties in ANS. In any event, our principal intent is to employ ANS as a probe of the role of "hydrophobicity" per se in both ANS binding and the fluorescence evinced, our ultimate aim being to study the role of solvent-water dynamics in the cavity. The principal focus in this discussion, however, is to rationalize our thermodynamic data on ANS binding in light of the optical spectroscopy and the known crystal structure.

Comparisons based on fluorescence spectroscopy

The λ_{max} for fluorescence of ANS in apomyoglobin is 454 nm (Stryer, 1965), 465 nm for the serum albumin-ANS complex (Weber and Laurence, 1954), ~480 nm in a polyclonal anti-ANS igG preparation (Parker and Osterland, 1970), ~484 nm in ANS-chymotrypsin (Weber et al., 1979), and 494 nm for ANS bound to tropomyosin (Oyashiki and Sekine, 1979). Thus the binding site for ANS in I-FABP, with a λ_{max} for bound ANS of ~480 nm, would seem to be among the more "polar" within this group of proteins. As in α-chymotrypsin (Johnson et al., 1979), the I-FABP binding site is apparently not anhydrous; ANS binds close to the amino terminus of the A chain of chymotrypsin (Weber et al., 1979). Although the ANS is thus fairly well solvent exposed, there are apparently ordered waters nearby in the α-chymotrypsin:ANS complex, as there may well be in I-FABP. Thus, although the presence of water in the binding site may affect the degree of blue-shift of the emission, relative to the fluorescence of ANS in pure water, the enhancement of the quantum yield of bound ANS appears to reside in other factors as well. One important factor may have to do with the restriction of the geometry of ANS when bound to the protein, compared with the conformational freedom of ANS in pure water.

Literature values of the quantum yield of ANS in H_2O are 0.003 (Robinson et al., 1978; Fœrster and Rokos, 1967), similar to our value of 0.0025. The apparently anomalous long radiative lifetime of ANS in water (108 ns versus 42 ns, from Eq. 3), and the isotope effect on k_{rad} in water, both of which disappear on the protein, require some comment. If one inspects the Einstein formula for k_{rad}, upon which the Strickler-Berg formula (Eq. 3) is based, it is difficult to envision how such an isotope effect might arise, unless the geometry of the radiating species is different in some isotopically sensitive way from the initially prepared excited state, i.e., because establishing this geometry requires solvent (H-bond) reorganization or proton motion. But this scenario is evidently not true of the protein-bound species, probably because binding interactions effectively freeze the ground- and excited-state geometries into coincidence. For example, in α-chymotrypsin (Weber et al., 1979) that conformation of ANS which maximizes van der Waals contact area for the phenyl was obtained by twisting the phenyl ring into a "high *syn*" (nearly orthogonal) conformation relative to the naphthyl. Such a conformation is similar to what Dodiuk et al. (1979) hypothesized was the case with the apomyoglobin-ANS complex. It may be that this "twist" is responsible for the observed long lifetimes in protein complexes and may also be the reason why the Strickler-Berg formula gives the correct prediction for the protein. Without any conformational restriction (as in water), there is a noncorrespondence of emissive state geometry with the geometry of the initially prepared excited state (cf. Douglas, 1966). On this interpretation, it is conceivable that the long lifetime and high quantum yield of 1,8-ANS in I-FABP are more a function of the geometrical constraints placed upon the conformatiuon of bound ANS by the binding site, rather than the "hydrophobicity" per se of the cavity. Thus, both albumin and apomyoglobin, which are more nonpolar than I-FABP on the basis of the maximum emission wavelength, vide supra, display a shorter fluorescence lifetime for bound ANS (~16 ns) than ANS-I-FABP, even as they display a longer fluorescence lifetime than that found for ANS in either dioxane or ethanol: that is, ~12 ns in both of these solvents (cf. Slavik, 1982). For the α-chymotrypsin complex, the actual electron density for the bound ANS was found to be axially symmetric about the N-$C_{1phenyl}$ bond (Weber et al., 1979), so that this hypothetical "twist" is probably not frozen in in that protein, but interestingly, the fluorescence lifetime of ANS in the chymotrypsin complex is also only 12 ns, compared with our value of 20 ns. Furthermore, as pHs increases from 3.5, the chymotrypsin-ANS complex loses up to 98% of its fluorescence at pH 3.5, and the emission spectrum resembles more and more that in water, whereas the binding constant for ANS is nearly unchanged ($K_d \approx 1 \times 10^{-4}$ M). Nonetheless, in the crystal, the fluorescence decay curves are very similar at pH 3.6 and pH 6.9, suggesting that crystal packing forces may operate to inhibit the "quenching" that occurs because of increased pH in solution. We will deal with these and other issues of ANS photophysics, specifically with respect to the altered properties of ANS observed upon binding to protein, more fully in a subsequent publication. The more relevant question at the moment concerns the various physicochemical contributors to the strength of the ANS–I-FABP interaction.

The contribution of hydrophobicity to I-FABP–ANS interaction

Because 1,8-ANS is amphiphilic in nature, possessing both a charged and an hydrophobic moiety, we can imagine that the free energy of hydration (or "proteination") for a compound A-B, where A is polar or charged, and B is hydrophobic, cannot in general be written as the simple additive interaction (Ben-Naim, 1983):

$$\Delta G(\text{A-B; protein} \leftarrow \text{water}) \tag{8a}$$

$$= \Delta G(\text{A; protein} \leftarrow \text{water}) + \Delta G(\text{B; protein} \leftarrow \text{water})$$

one of which is the "electrostatic" and the other the "hydrophobic" interaction, but rather, we can write the total free energy as an additive function of conditional free energies:

$$\Delta G(\text{A-B; protein} \leftarrow \text{water}) \tag{8b}$$

$$= \Delta G(\text{A; protein} \leftarrow \text{water}) + \Delta G(\text{B; protein} \leftarrow \text{water| A})$$

the difference lies in the second term, which is the conditional free energy of binding B to the protein, in the presence of bound A. We note in passing that, although formally we could equally have written the ΔG(A-B; protein←water) as a sum of the free energy for binding B to the unperturbed protein and the conditional free energy of binding A in the presence of pre-bound B, in the actual physical situation these are not the same processes. Because the anion binding site is buried, it is likely to be the case that the sulfonate moiety is attracted to its site first, whereas the aryl rings find their equilibrium relative twist subsequently. The inverse process (binding by the rings first, and then the sulfonate finding the buried arg-106) seems unlikely. In this section we focus on the second term, the conditional hydrophobic interaction.

The so-called direct hydrophobic effect itself has been elucidated in terms of the solute-solute pair correlation function for apolar molecules in aqueous environments. Pratt and Chandler (1977), derived this from consideration of the cavity:cavity pair correlation function in water. They obtained an expression for this function by means of the empirical water:water correlation function (one can think of their procedure as finding the "holes" in the water:water correlation function via a switching off of the intermolecular potential). The pair correlation function for hard spheres is then grafted onto the cavity:cavity correlation function in the short-range region, where one expects repulsion between two apolar solutes to dominate (because cavities do not repel). With no adjustable parameters, their apolar pair correlation function could explain such classical expressions of direct hydrophobic interaction as the tendency of two apolar molecules, for example two hexanes, to associate in water. In a subsequent refinement, attractive interactions were incorporated in the theory as a perturbation of the long-range tail of the apolar correlation function to mimic electrostatic or van der Waals forces between the apolar species (Pratt and Chandler, 1980). This perturbation, a small change in the molecular force field, could then allow for the differences in the degree of association of two hexanes versus that of two benzenes, or even versus that of two pentanol molecules. Thus, a conditional hydrophobic interaction can be said to occur when this perturbation becomes very large, as in the case of surfactants (Oakenfull and Fenwick, 1975), which have charged headgroups that can effectively alter the water:water correlation function in their vicinity. Because the apolar correlation function is ultimately derived from the water correlation function, the new apolar correlation function that characterizes this conditional hydrophobic interaction is drastically altered from the original. I-FABP consists of what is essentially a preformed cavity in water, since, although it is filled with waters, these are bounded by the protein structure. This does not mean that there is no exchange with bulk water, or even that this exchange is necessarily slow with respect to self-diffusion rates in bulk water, but rather that the number of hydrogen bond connections from cavity waters that extended to large distances into the bulk-water phase is small, compared with the size of these networks in the bulk phase. There is an effective switching off of the water-water potential of mean force at these large distances, and hence a cavity, i.e., a place where ANS can go. The presence of this cavity, possessing a long-range sulfonate-attracting feature inside it (arg-106), means that it should be legitimate to continue to refer to I-FABP–ANS binding as a predominantly (even though conditional) hydrophobic effect, despite the large amount of water present in the apoprotein.

The near-constancy of isotope effect on the binding affinity of I-FABP for ANS, despite large overall changes in affinity at differing pHs, can be explained if the conditional free energy of the hydrophobic contribution to binding were isotopically sensitive, and the electrostatic contribution were not. Then:

$$\Delta G(\text{D}) - \Delta G(\text{H}) = \delta G_{\text{HI,D}} - \delta G_{\text{HI,H}} \approx -RT \ln 3 \tag{9}$$

where ΔG(D) is the binding free energy for ANS in D_2O, $\delta G_{\text{HI,D}}$ is the conditional hydrophobic interaction for ANS in D_2O (i.e., the hydrophobic interaction in the presence of the charged group cf Ben-Naim, 1983), and H's signify the same quantities in H_2O. In fact, isotopic sensitivity of the hydrophobic effect is not surprising from the Pratt-Chandler view, whereas isotopic differences in, e.g., the free energy of ionic hydration, are usually rather small (Friedman and Krishnan, 1973). This insensitivity of part of the interaction (the electrostatic part, which titrates, i.e., which has a pH dependence) to isotopic substitution, while the other part maintains a nearly constant difference between the two waters, is very good prima facie evidence for the validity of the formal separation of hydrophobic/electrostatic contributions we propose above. Although it has been established (as described by Ben-Naim, 1983) by a number of measures that the so-called direct hydrophobic interaction, i.e., the

effective attraction between hydrophobic solutes in aqueous solution, is weaker in D_2O than H_2O, measurements for conditional hydrophobic interaction such as that involved here show that it is *stronger* in D_2O than H_2O. Thus, Oakenfull and Fenwick (1975) showed that the binding of alkyl-carboxylates into micelles made up of alkyl chains with both anionic and cationic head groups was favored in D_2O by an amount corresponding to -0.9 kcal/mol per methylene group, for chains containing more than 6 $-CH_2-$ moieties. Similarly, these authors also showed that a hydrophobic effect could effectively accelerate an amidation reaction by allowing general base catalysis from a second alkylamine molecule, which is attracted to the neighborhood of the first by the hydrophobic effect. A solvent isotope effect is observed in this system (Oakenfull and Fenwick, 1975), which suggests that the conditional hydrophobicity for the given alkylamines is ~1.8 kcal/mol stronger in D_2O than H_2O. As we have discussed, what we observe in I-FABP is also not a classical type of hydrophobicity, that is, the aromatic ring system of ANS binds in the presence of a sulfonate. Both the direction and the magnitude of the isotope effects in these model systems are similar to our results. There is no general agreement on an explanation for this reversal of isotope effects conditioned by the presence of a charged moiety on a hydrophobic solute.

The electrostatic contribution to I-FABP:ANS affinity

Our experiments with the effect of ionic strength yielded a value for the slope of log K_d versus $\sqrt{I}$ of 2.6 ± 0.5. This should not be taken as an indication that the effective charge of I-FABP as seen by ANS is ~+2.6. The actual charge on I-FABP at any pH used in this study is negative, not positive. An alternative explanation for the observed slope arises out of the fact that the screening of charge is fairly effective even at the lowest salt concentrations used. It appears that even at 10 mM added salt, the Debye screening length is roughly 30 Å (Bockris and Reddy, 1977), so that the ANS anion and some cationic species in I-FABP (i.e., the most significant one for binding ANS), presumably arg-106, can effectively interact only when they are in fairly close proximity. Perhaps the ANS can only become influenced by the charge buried within the cavity when it diffuses close to the entrance, nearly 25 Å from the arg-106. If such is the case, the observed slope may be an indication that the effective dielectric constant within the cavity is ~42 ± 8, not ~80 as in bulk water, despite the water present in the apoI-FABP, because it is the screening by real and virtual ions carried into the cavity by solvent that is, in our view, the relevant modulation of the electrostatic interaction probed by our varying I. We obtain this value of ϵ by inverting Eq. 6 into a formula for ϵ in terms of the other parameters and the ratio of the observed slope of log K_d versus $\sqrt{I}$ (2.6) to the expected slope for a 1:1 interaction in water, 1.02, and the expected dielectric constant in water, 78. If we include the buffer-effect correction mentioned above, the value is ~38 for ϵ. This value of ϵ is similar to that of acetonitrile or DMF, and is appreciably more polar than the value expected for hydrophobic protein interiors (<10, but cf. Warshel, 1987).

A model for the observed changes in heat capacity upon ANS binding

The large decrease in entropy associated with the binding event at higher pHs and temperatures as well as the changes in $\Delta H°$ can be subsumed into the observed large negative change in heat capacity upon ligand association. It is this ΔC_p that Fig. 9 is meant to explain. Initially, the protein cavity is filled with water. The protein backbone experiences stronger hydrogen bonding to water than to peptides (or protein, etc.; cf. Connelly et al., 1994), so that the strength of interactions will in general be stronger for protein-to-water than protein-to-ligand interac-

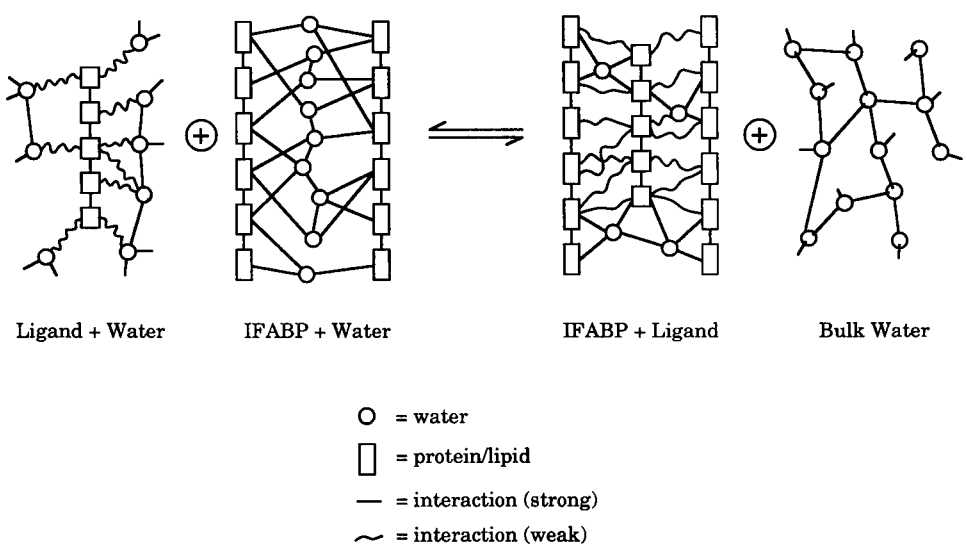

FIGURE 9 Schematic diagram displaying our proposed explanation of the large negative heat capacity of ligand binding, $\Delta C_{p,\ ligand}$. Small circles represent water molecules, large blocks are elements of the protein structure, small squares represent lipid (or ANS) moieties. Straight, bold lines represent strong interactions (hydrogen or covalent bonds); wavy lines, weak interactions (weak hydrogen bonds, van der Waals forces, etc.).

tions. In addition, the cavity-water experiences more strong interactions on average than are present in bulk water (in the figure, ~3 versus ~2 in bulk) (Rahman and Stillinger, 1971; cf. also Finney, 1979), which can be responsible for the positional order found in the crystal structure. This large number of interactions would generate a large number of states of the protein + water system within kT of the most stable state, which multiplicity is responsible for the heat capacity (and hence entropy changes) in the system. In contrast, after ligand is bound, the geometry of the complex is rather fixed (constrained), as is the configuration of the remaining waters. The water in the I-FABP cavity ought then to be bound tightly (more so after than before ligand is bound), and this tightness ought to oppose the binding process. But the water that is lost upon binding is also to a large extent tightly bound to itself, and the internal hydrogen bond network of the cavity might collapse in stages upon binding. Such a process might be manifested in the difference between the van't Hoff and calorimetric enthalpies. Water bound to ligand also experiences a negative change in heat capacity on being released to the bulk phase (cf. Privalov and Gill, 1988), also presumably because of the large number of isoergonic configurations available to it. But this water is more strongly bound in its final state (the bulk phase), so the net (hydrophobic) driving force for the binding could be the release of this water. The heat capacity changes for the solution of benzene and alkyl benzenes from water to the organic phase (Privalov and Gill, 1988) are, in fact, on the same order of magnitude as we observed here, ~ -300 cal/deg-mol, and there appears to be a break in this $\Delta C_{p\ sol}$ about 35°C. Although this is an intriguing result, it is not clear to what extent these compounds are relevant to the heat capacity of transfer of ANS (e.g., the solubility of the ammonium salt of ANS in water is at least 15 times that of benzene, ANS is not purely apolar) or to what extent the transfer to organic phase actually resembles the transfer to the protein cavity (with $\epsilon \approx 40$). As we have displayed it in the figure, the ligand also has more (although weak) interactions when bound to protein than when in solution, and so these would also contribute to the observed enthalpy of binding, but there is no direct evidence for this, unless we invoke the fluorescence lifetime data of the bound ANS, which implied that the geometry is constrained.

From Table 2, 20.5 cal/deg-mol of entropy are lost in the process (at pH 7.53):

$$\Delta S^\circ\{[\text{I-FABP–ANS complex 8°C} \rightarrow \text{I-FABP–ANS complex 30°C}\} \quad (10a)$$
$$- \Delta S^\circ\{[\text{I-FABP + ANS}|H_2O\ 8°C \rightarrow \text{I-FABP + ANS}|H_2O\ 30°C\}.$$

This entropy, defined as

$$\Delta\Delta S^\circ = \Delta \int đq_{rev}/T, \quad (10b)$$

should be equal to

$$\int C_p(\text{I-FABP–ANS complex})dT/T - \int C_p(\text{I-FABP,free + ANS, free})dT/T = \int \Delta C_p d \ln T; \quad (10c)$$

From our data, $\Delta C_p = -283$ cal/deg-mol, whereas $\Delta \ln T = 0.0743$, thus $\Delta\Delta S^\circ$ should be -21 cal/deg-mol, very close to our observed value. This analysis demonstrates an important point: the ΔH° values and the ΔG° values we obtained are mutually consistent when compared in this manner, i.e., by comparing the slope of the ΔH° versus T curve, versus the difference between two temperatures of the difference between ΔG°—which is obtained from fluorimetry—and ΔH°, i.e., $\Delta S^\circ_{22°C} - \Delta S^\circ_{8°C}$.

We have mentioned that the waters in the apoprotein are ordered crystallographically. This fact does not necessarily imply, as we have intimated above, that the residence time of water in the protein cavity is especially long (Levitt and Park, 1993), or that the ANS-binding event, for example, is rate limited by the off-rate of waters in the cavity exchanging with bulk. It means strictly that the positions of oxygen atoms in the cavity in one unit cell will be highly correlated with the positions of the oxygen atoms at another unit cell in the crystal, or at another time. Water can still flow into and out of the cavity, as well as within it. But the "new" oxygen atoms will on the average take up the same positions as were occupied by the old oxygen atoms. This positioning effect is induced by the environment, the highly asymmetrical positions of possible interacting atoms belonging to the protein. Packing forces could themselves slow down the diffusion into and out of the cavity in the crystal, but slow diffusion of cavity-water need not be a feature present in solution. Diffusion constants are given by the velocity autocorrelation function (Hertz, 1977). The decay constant of the positional autocorrelation function for waters in the cavity would be related to the residence time on sites for these cavity waters. A site autocorrelation function would decay with a constant characterizing the "disordering time" for the order observed crystallographically, and it is this time that would be very long. Thus there need not be any direct relationship between these three "times" because the underlying correlation functions are very different.

Fig. 9 suggests how the excess heat capacity observed in the initial state of the system (i.e., [solvated protein] + [solvated ligand], relative to the final state of [ligand-pro-

tein] + [water released into bulk]) might come about. Water has a large heat capacity compared with nearly all other liquids, so evidently hydrogen bonds contribute more to heat capacity than weaker van der Waals interactions. It becomes an important feature in the figure that the apoprotein carries so many hydrogen bonds, both from water to protein and to other cavity water. It is the loss of these hydrogen bonds that we believe is mostly responsible for the negative ΔC_p observed. But although the oxygen positions could be fairly constrained, the hydrogen bond pattern may still be fairly disordered. Although the degree of organization of water in the cavity may differ from bulk (Chevernak and Toone, 1994), it remains possible that cavity-water exchange with bulk water may not be rate-determining for ANS binding. Hence, it might also be difficult to find any ANS-displaceable water molecules with exceptionally long residence or correlation times in the protein cavity from NMR experiments (cf. Ernst et al., 1995).

SUMMARY AND CONCLUSIONS

We have investigated the binding to I-FABP of 1,8-ANS by a variety of techniques. We report here on the thermodynamics ($\Delta G°$, $\Delta H°$, and $\Delta S°$) of ANS binding as obtained from steady-state fluorescence and calorimetric techniques. The binding at all temperatures is enthalpically driven, and it is entropically opposed at all temperatures above 14°C (below this temperature there is a positive contribution by the entropy). The changes with temperature of the binding enthalpy and entropy are apparent from the (negative) changes in heat capacity upon binding. To further elucidate the source of the driving forces for the binding event, the solvent isotope effect on this system was measured at a variety of pH/pD values, together with the salt dependence of the affinity constant. These data suggested that the binding energy involves contributions from both electrostatic and conditional hydrophobic interactions. Most of the latter could be explained by the release of cavity water and/or ligand-associated water upon binding. The salt dependence of the binding constant, together with the fluorescence data, further suggests that the binding site is comparatively polar in nature, with $\epsilon \approx 42$, consistent with the persistence of some water molecules after ANS binding. The changes in heat capacity we think are due to a net loss in the thermally available number of hydrogen bond states for the relatively ordered cavity waters upon their release into the bulk. Last, the fluorescence, absorption, and fluorescence lifetime analysis suggested that bound excited-state ANS undergoes no substantial conformational rearrangement during its lifetime, suggesting some rigidity in bound ANS on this (20 ns) time scale, as opposed to the situation likely to exist in aqueous solution.

We wish to thank William Wessels for assisting in the lifetime measurements, Peter Callahan for assistance with the figures, Ben Madden for amino acid analysis, and Michael Rogers for his advice with the expression of the protein.

Supported by National Institutes of Health grant GM 34847.

REFERENCES

Banaszak, L., N. Winter, Z. Xu, D. Bernlohr, S. Cowan, and T. Jones. 1994. Lipid-binding proteins: a family of fatty acid, and retinoid binding proteins. *Adv. Prot. Chem.* 45:89–151.

Ben-Naim, A. 1983. Hydrophobic Interactions. Plenum Press, New York.

Bockris, J., and A. Reddy. 1977. Modern Electrochemistry. Plenum Press, New York.

Brand, L., and B. Witholt. 1967. Fluorescence measurements. *Methods Enzymol.* 11:776–856.

Brandts, J. 1993. ITC Data Analysis in Origin, Appendix. Microcal Systems, Northampton, MA.

Cantor, C., and P. Schimmel. 1980. Biophysical Chemistry, Part II. W. H. Freeman, New York.

Chevernak, M., and E. Toone. 1994. A direct measurement of the contribution of solvent reorganization to the enthalpy of ligand binding. *J. Am. Chem. Soc.* 116:10533–10539.

Connelly, P., R. Aldape, F. Bruzzese, S. Chamber, M. Fitzgibbon, M. Fleming, S. Itoh, D. Livingston, M. Navia, J. Thomson, and K. Wilson. 1994. Enthalpy of hydrogen bond formation in a protein-ligand binding reaction. *Proc. Natl. Acad. Sci. USA.* 91:1964–1968.

Cornish-Bowden, A. 1995. Analysis of Enzyme Kinetic Data. Oxford University Press, Oxford.

Demas, J., and G. Crosby. 1971. The measurement of photoluminescence quantum yields: a review. *J. Phys. Chem.* 75:991–1024.

Dill, K. 1990. The meaning of hydrophobicity. *Science.* 250:297.

Dodiuk, H., H. Kanety, and E. Kosower. 1979. The apomyoglobin-arylaminonaphthalene-sulfonate system. insight into fluorescent probe responses by substituent modulation. *J. Phys. Chem.* 83:515–521.

Douglas, A. 1966. Anomalously long radiative lifetimes of molecular excited states. *J. Chem. Phys.* 45:1007–1015.

Ernst, J., R. Clubb, H.-X. Zhou, A. Gronenborn, and G. Clore. 1995. Demonstration of positionally disordered water within a protein hydrophobic cavity. *Science.* 267:1813–1817.

Finney, J. 1979. The organization of water in protein crystals. *In* Water: A Comprehensive Treatise, Vol. 6. F. Franks, editor. Plenum Press, New York. 47–122.

Fœrster, T., and K. Rokos. 1967. A deuterium isotope solvent effect on fluorescence. *Chem. Phys. Lett.* 1:279–280.

Franks, F. 1975. The hydrophobic effect. *In* Water: A Comprehensive Treatise, Vol. 4. F. Franks, editor. Plenum Press, New York. 1–115.

Friedman, H., and C. Krishnan. 1973. Thermodynamics of ionic hydration. *In* Water: A Comprehensive Treatise, Vol. 3. F. Franks, editor. Plenum Press, New York. 1–118.

Goldberg, M., G. Semisotnov, B. Friguet, K. Kuwajima, O. Ptitsyn, and S. Sugai. 1990. An early immunoreactive folding intermediate of the tryptophan synthase $\beta 2$ subunit is a "molten globule." *FEBS Lett.* 263: 51–56.

Guilbault, G. 1973. Practical Fluorescence: Theory, Methods and Techniques. Marcel Dekker, New York.

Hertz, H. 1977. Velocity correlations in aqueous electrolyte solutions from diffusion, conductance and transference data. Part 1. Theory. *Ber. Bunsenges. Physik. Chemie.* 81:656–674.

Jakoby V. M., K. Miller, J. Toner, A. Bauman, L. Cheng, E. Li, and D. Cistola. 1993. Ligand-binding electrostatic interactions govern the specificity of retinol- and fatty acid-binding proteins. *Biochemistry.* 32: 872–878.

Jencks, W. 1975. Binding energy, specificity, and enzymic catalysis. *Adv. Enzymol. Relat. Areas Mol. Biol.* 43:219–410.

Johnson, J., M. El-Bayoumi, L. Weber, and A. Tulinsky. 1979. Interaction of α-chymotrypsin with the fluorescent probe 1-anilinonaphthalene-8-sulfonate in solution. *Biochemistry.* 18:1292–1295.

Kirk, W., E. Kurian, and F. Prendergast. 1995. Thermodynamics of (1, 8) ANS binding to intestinal fatty acid binding protein (IFABP). *Biophys. J.* 68:A196.

Kirk, W., W. Wessels, and F. Prendergast. 1993. Lanthanide-dependent perturbations of luminescence in indolylethylenediaminetetraacetic acid-lanthanide chelate. *J. Phys. Chem.* 97:10326–10340.

Kirkwood, J. 1934. Theory of solutions of molecules containing widely separated charges with special application to zwitterions. *J. Chem. Phys.* 3:351–360.

Klotz, I. 1982. Number of receptor sites from scatchard graphs: facts and fantasies. *Science.* 217:1247–1250.

LaLonde, J., M. Levenson, J. Roe, D. Bernlohr, and L. Banaszak. 1994. Adipocyte lipid binding protein complexed with fatty acid. *J. Biol. Chem.* 269:25339–25347.

Levitt, M., and B. Park. 1993. Water: now you see it, now you don't. *Structure.* 1:223–226.

Marcus, R. A. 1965. On the theory of electron transfer reactions. VI. Unified treatment for homogeneous and electrode reactions. *J. Chem. Phys.* 43:679–701.

Nemethy, G., and H. Scheraga. 1962. The structure of water and hydrophobic bonding in proteins. III. The thermodynamic properties of hydrophobic bonds in proteins. *J. Phys. Chem.* 66:1773–1789.

Oakenfull, D., and D. Fenwick. 1975. Hydrophobic interaction in deuterium oxide. *Aust. J. Chem.* 28:715–720.

O'Connor, D., and W. Ware. 1976. Exciplex photophysics. III. Kinetics of fluorescence quenching of α-cyanonaphthalene by dimethylcyclopenten-1,2 in hexane. *J. Am. Chem. Soc.* 98:4706–4709.

Okubo, T., and N. Ise. 1969. The solubilities of naphthalene and biphenyl in aqueous polymer solutions. *J. Phys. Chem.* 73:1488–1494.

Oyashiki, T., and T. Sekine. 1979. Fluorometric studies on conformational changes in tropomyosin associated with depolymerization. *J. Biochem.* 85:575–580.

Parker, C., and C. Osterland. 1970. Hydrophobic binding sites on immunoglobulins. *Biochemistry.* 9:1074–1082.

Pratt, L., and D. Chandler. 1977. Theory of the hydrophobic effect. *J. Chem. Phys.* 67:3683–3703.

Pratt, L., and D. Chandler. 1980. Effect of solute-solvent attractive forces on hydrophobic correlations. *J. Chem. Phys.* 73:3434–3441.

Privalov, P., and S. Gill. 1988. Stability of protein structure and hydrophobic interaction. *Adv. Protein Chem.* 39:191–234.

Rahman, A., and F. Stillinger. 1971. Molecular dynamics study of liquid water. *J. Chem. Phys.* 55:3336–3348.

Richieri, G., R. Ogata, and A. Kleinfeld. 1992. A fluorescently labeled intestinal fatty acid binding protein. Interactions with fatty acids and its use in monitoring free fatty acids. *J. Biol. Chem.* 267:23495–23501.

Robinson, G., R. Robbins, G. Fleming, J. Morris, A. Knight, and B. Morrison. 1978. Picosecond studies of the fluorescent probe molecule 8-anilino-1-naphthalenesulfonic acid. *J. Am. Chem. Soc.* 100: 7145–7150.

Sacchettini, J., L. Banaszak, and J. Gordon. 1990. Expression of rat intestinal fatty acid binding protein in *E. coli* and its subsequent structural analysis: a model system for studying the molecular details of fatty acid-protein interaction. *J. Mol. Cell. Biochem.* 98:81–93.

Sacchettini, J. C., J. I. Gordon, and L. J. Banaszak. 1989. Crystal structure of rat intestinal fatty-acid-binding protein. Refinement and analysis of the *Escherichia coli*-derived protein with bound palmitate. *J. Mol. Biol.* 208:327–339.

Sambrook, J., E. Fritsch, and T. Maniatis. 1989. Molecular Cloning: A Laboratory Manual, 2nd Ed., Vol 3. Cold Spring Harbor Laboratory, Plainview, NY.

Scapin, G., J. Gordon, and J. Sacchettini. 1992. Refinement of the structure of recombinant rat intestinal fatty acid binding protein at 1.2 Å resolution. *J. Biol. Chem.* 267:4253–4269.

Sirangelo, I., E. Bismuto, and G. Irace. 1994. Solvent and thermal denaturation of the acidic compact state of apomyoglobin. *FEBS Lett.* 338: 11–15.

Slavik, J. 1982. Anilinonaphthalene sulfonate as a probe of membrane composition and function. *Biochim. Biophys. Acta.* 694:1–25.

Strickler, S., and R. Berg. 1962. Relationship between absorption intensity and fluorescence lifetime of molecules. *J. Chem. Phys.* 37:814–822.

Stryer, L. 1965. The interaction of a naphthalene dye with apomyoglobin and apohemoglobin. A fluorescent probe of nonpolar binding sites. *J. Mol. Biol.* 13:482–495.

Tanford, C. 1973. The Hydrophobic Effect. Wiley, New York.

Warshel, A. 1987. What about protein polarity? *Nature.* 330:15–16.

Weber, G. 1952. Polarization of the fluorescence of macromolecules. 2. Fluorescent conjugates of ovalbumin and bovine serum albumin. *Biochem. J.* 51:155–167.

Weber, G., and D. Laurence. 1954. Fluorescent indicators of adsorption in aqueous solution and on the solid phase. *Biochem. J.* 56:xxxi.

Weber, L., A. Tulinsky, J. Johnson, and M. El-Bayoumi. 1979. Expression of functionality of α-chymotrypsin. The structure of a fluorescent probe-α-chymotrypsin complex and the nature of its pH dependence. *Biochemistry.* 18:1297–1303.

Xu, Z., M. Buelt, L. Banaszak, and D. Bernlohr. 1991. Expression, purification, and crystallization of the adipocyte lipid binding protein. *J. Biol. Chem.* 266:14367–14370.

Yang, M., S. Ghosh, and D. Millar. 1994. Direct measurement of thermodynamic and kinetic parameters of DNA triple helix formation by fluorescence spectroscopy. *Biochemistry.* 33:15329–15337.